

PACS numbers: 42.55.Ks; 42.60.Lh
DOI: 10.1070/QE2008v038n10ABEH013864

Simulation of a two-frequency cw chemical HF – HBr laser

B.P. Aleksandrov, B.I. Katorgin, A.A. Stepanov

***Abstract*. An autonomous cw chemical HF – HBr laser emitting simultaneously at ~2.7 μm (HF molecules) and ~4.2 μm (HBr molecules) is studied numerically by using complete Navier – Stokes equations. It is shown that the output power of the HBr laser per unit area of the nozzle array can achieve ~20 W cm^{-2} for the laser region length ~20 cm. The relation between the radiation intensities emitted by HF and HBr molecules is controlled by diluting the secondary fuel by bromine.**

Keywords: *cw chemical laser, two-frequency lasing, gas-dynamic Navier – Stokes model.*

1. Introduction

Continuous wave chemical lasers (CCLs) operating simultaneously on two different molecules attract interest because they can be used for the development of high-power radiation sources emitting at frequencies lying in different spectral regions. Such lasers can find a variety of applications related, in particular, to the propagation of radiation through the atmosphere, the interaction of radiation with various materials, and in chemical and laser technologies, laser locations and communications, remote gas analysis of the environment, etc. The possibility of obtaining simultaneous cw lasing was theoretically investigated for the HF – HCl [1], DF – CO_2 [2], and HF – DF [3, 4] molecular pairs.

The two-frequency operation regime of a CCL can be obtained by using the class of exothermal chemical reactions of the type

$$A + BC \xrightarrow{k_1} AB^* + C,$$

$$A + BC \xrightarrow{k_2} AC^* + B,$$

in which vibrationally excited molecules are produced simultaneously via two channels. It is important that the rate constants k_1 and k_2 in both channels should be large enough and the energy release in each of the channels would be sufficient for the inverse population of vibrational levels of the produced molecules. Such reactions include, for example, reactions with the participation of hydrogen atoms (or its heavier isotope – deuterium) and halogen molecules, in particular, ClF, BrF, BrCl and others.

The two-dimensional model of a two-frequency HF – HBr laser was developed in [5] based on 'narrow channel' equations. The laser had the scheme of a conventional HF laser in which Br_2 molecules were added to molecular hydrogen in the secondary fuel flow. The authors of paper [5] calculated the operation of a small-scale laboratory laser described in [6] and showed that a HF – HBr laser differs from a HF laser by a more intense heat release, which reduces the gain in the active medium at the emission frequencies of HF molecules. The gain at the emission frequencies of HBr molecules proved to be an order of magnitude lower than at the emission frequencies of HF molecules.

In this paper, we calculated the operation of a cw HF – HBr laser with a slot nozzle array with a step of 7 mm. The calculations were performed by using the model based on complete Navier – Stokes equations. This model allows the detailed study of regimes with transverse pressure gradients and compression jumps and normal shocks, which are typical for flows with a strong heat release.

2. Mathematical model

The geometry of jet flows in the active region of many CCLs is two-dimensional as, for example, in the generators of the active medium with the planar or cylindrical slot design of a nozzle unit. Below, we present the two-dimensional mathematical model of the active medium for lasers of this type. For generality, we consider the cylindrical generator (of radius r_0) of the active medium of an autonomous CCL (Fig. 1) whose planar construction is a particular case of the cylindrical construction of a large radius. The nozzle unit of the CCL of this type is an array of many alternating coaxial oxidiser and fuel supersonic nozzles. The jets are pumped in the radial direction. The mixing of jets and propagation of radiation occur along the cylinder axis z. The sizes of the oxidiser and fuel flows along the z axis on the nozzle unit surface are denoted by h_1 and h_2, respectively, and the period of the nozzle array is $h \equiv 2h^* = h_1 + h_2$.

We calculated lasing for the case of a plane – parallel Fabry – Perot resonator formed by circular mirrors, in

B.P. Aleksandrov, B.I. Katorgin, A.A. Stepanov V.P. Glushko Energomash Research and Production Association, Open Joint-Stock Company, ul. Burdenko 1, 141400 Khimki, Moscow region, Russia; e-mail: energo@online.ru

Received 9 April 2008
Kvantovaya Elektronika **38** (10) 903 – 908 (2008)
Translated by M.N. Sapozhnikov

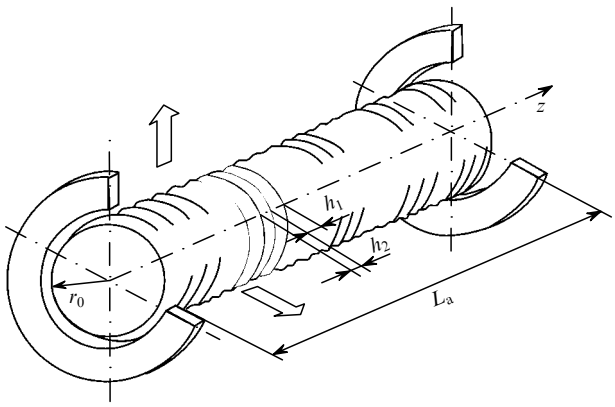

Figure 1. Sketch of the modelled cylindrical generator of the CCL active medium.

which an active medium of length L_a was placed. If the reflectivities of mirrors are approximately equal, the inhomogeneity of the field along the z axis inside the resonator can be neglected. In this case, the problem can be solved by considering the region $0 \leqslant z \leqslant h^*$ between the symmetry planes of fuel and oxidiser nozzles.

The CCL model is based on the complete system of two-dimensional Navier–Stokes equations for the flow of a multicomponent chemically active vibrationally nonequilibrium gas mixture in the presence of resonance radiation. The stationary distribution of the flow parameters is found by solving the nonstationary system of equations by the stabilising method. The gas mixture consists of $N_c = \sum_k N_{v_k}$ components, including molecules in different vibrational states (having the equilibrium distribution over rotational quantum states), where N_{v_k} is the number of vibrational levels of the kth molecule).

The system of nonstaionary Navier–Stokes equations can be written in the tensor form [7–10]

$$\frac{\partial \rho}{\partial t} + \nabla(\rho \boldsymbol{V}) = 0,\ \frac{\partial \rho V_\alpha}{\partial t} + \nabla(\rho \boldsymbol{V} V_\alpha) - (\nabla \cdot \hat{\sigma})_\alpha = -(\nabla p)_\alpha,$$

$$\frac{\partial(\rho E)}{\partial t} + \nabla(\rho E \boldsymbol{V} + \boldsymbol{q}) = -p\nabla \boldsymbol{V} + (\hat{\sigma} \cdot \nabla)\boldsymbol{V} - \sum_k \sum_{v=1}^{N_{v_k}} g_v I_v,$$

$$\frac{\partial \rho c_k}{\partial t} + \nabla(\rho \boldsymbol{V} c_k) + \nabla \boldsymbol{j}_k = \dot{w}_k + \frac{W_k}{N_A}\left(\frac{g_{v+1+l} I_{v+1+l}}{h\nu_{v+1+l}} - \frac{g_v I_v}{h\nu_v}\right),$$

$$k = 1, \ldots, N_c,$$

where

$$\nabla = \boldsymbol{i}\frac{\partial}{\partial x} + \boldsymbol{j}\frac{\partial}{\partial y} + \boldsymbol{k}\frac{\partial}{\partial z}$$

is the symbolic nabla vector; $\alpha = r, z$;

$$p = \frac{\rho R T}{W};\ W = \left(\sum_{k=1}^{N_c} \frac{c_k}{W_k}\right)^{-1};\ E = \sum_{k=1}^{N_c} e_k c_k;$$

$$e_k = \int c_{vk}(T)\mathrm{d}T + h_{k0} + e_k^{\mathrm{vib}};\ \boldsymbol{q} = -\lambda \nabla T + \sum_{k=1}^{N_c} h_k \boldsymbol{j}_k;$$

$$h_k = h_{k0} + \int c_{pk}\mathrm{d}T + e_k^{\mathrm{vib}};\ \boldsymbol{j}_k = -\frac{\rho}{B_k}\nabla c_k + \boldsymbol{\delta}_k;$$

$$B_k = \sum_{i=1}^{N_c} \frac{W}{W_i}\frac{c_i}{D_{ki}};$$

$$\boldsymbol{\delta}_k = \frac{W c_k}{B_k}\sum_{i=1}^{N_c}\left(\frac{1}{W_i D_{ki}} - \frac{1}{W_k D_{kk}}\right)\boldsymbol{j}_i + \frac{\rho W c_k}{B_k}\nabla\left(\frac{1}{W}\right).$$

The lasing regime was calculated by using the approach of quasi-stationary generation for the vibrational–rotational transitions of the P branch (assuming that the parameters of the Fabry–Perot resonator mirrors are independent of the radiation frequency):

$$\int_0^{L_a} g_v \mathrm{d}z = -0.5 \ln(r_1 r_2).$$

In the equations presented above, ρ, p, $\boldsymbol{V}$, and T are the density, pressure, velocity and temperature of the gas mixture, respectively; E is the internal energy of the unit mass of the mixture; c_k is the mass fraction of the kth component in the mixture; $\sigma_{\alpha\beta}$ are components of the viscous stress tensor $\hat{\sigma}$ (neglecting the second viscosity); W_k, h_k, h_{k0}, c_{pk}, and c_{vk} are the molecular weight, specific enthalpy, the enthalpy of formation in the ground quantum state, the heat capacities of the kth component at constant pressure and constant volume, respectively; e_k^{vib} is the specific energy of the vibrational state; λ is the heat conductivity; D_{ki} is the binary diffusion coefficient; $\dot{w}_k$ is the rate of changing of the density of the kth component during chemical and vibrational processes; ν_v, g_v, and I_v are the frequency of the vibrational–rotational transition in the $v \to v-\ 1-l$ band, the local gain, and the radiation intensity at this transition, respectively; l is the overtone number; r_1 and r_2 are the reflectances of the resonator mirrors; and L_a is the active medium length along the optical axis.

The problem was solved in cylindrical coordinates r and z in the region $0 \leqslant z \leqslant h^*$, $r_0 \leqslant r \leqslant r^*$, $t \geqslant 0$. The boundary conditions in the symmetry planes $z = 0$, $z = h^*$ have the form

$$V_z = 0,\ \frac{\partial \rho}{\partial z} = \frac{\partial V_r}{\partial z} = \frac{\partial E}{\partial z} = \frac{\partial c_k}{\partial z} = 0.$$

At the boundary $r = r_0$ the profiles $f(r_0, z) = f_0(z)$ of all the variables of the problem were specified, which were found by calculating the oxidiser and fuel flows in nozzles by using the two-dimensional gas-dynamic 'narrow channel' model [11]. At the boundary $r = r^*$, the 'soft' boundary conditions $\partial^2 f/\partial r^2 = 0$ were used for the supersonic flow.

The stationary solution of the system of equations was obtained by the finite-difference method by using the splitting of differential operators over physical processes and spatial directions [12]. The accuracy of the solution convergence $\varepsilon = 10^{-3}$ specified in all calculations was sufficient for determining the exact solution, as was found in practice.

We used the kinetic model of the HF laser proposed in [13], the kinetic model of the HBr laser was described in detail in [5]. Here, we will present only chemical reactions in which vibrationally excited HF(v) and HBr(v) molecules are produced:

$$F + H_2(v = 0) \rightarrow HF(v \leqslant 3) + H,\ \Delta H = -32\ \text{kcal mol}^{-1}, \quad (1)$$

$$F + Br_2 \rightarrow Br + BrF,\ \Delta H = -14\ \text{kcal mol}^{-1}, \quad (2)$$

$$H + F_2 \rightarrow HF(v \leqslant 8) + F,\ \Delta H = -98\ \text{kcal mol}^{-1}, \quad (3)$$

$$Br + F_2 \rightarrow F + BrF,\ \Delta H = -22\ \text{kcal mol}^{-1}, \quad (4)$$

$$H + Br_2 \rightarrow HBr(v \leqslant 6) + Br,\ \Delta H = -41\ \text{kcal mol}^{-1}, \quad (5)$$

$$H + BrF \rightarrow HF(v \leqslant 7) + Br,\ \Delta H = -79\ \text{kcal mol}^{-1}, \quad (6)$$

$$H + BrF \rightarrow HBr(v \leqslant 4) + F,\ \Delta H = -31\ \text{kcal mol}^{-1}, \quad (7)$$

$$F + HBr \rightarrow HF(v \leqslant 4) + Br,\ \Delta H = -48\ \text{kcal mol}^{-1}. \quad (8)$$

3. Results of calculation and discussion

We investigated the HF–HBr CCL with a plane nozzle array of the slot type with the step $h = 7$ mm. The oxidiser nozzle length along the flow was assumed equal to 12 mm, the ratio of the output cross sections of the oxidiser and fuel nozzles was 3 : 1, and the degree of extension of oxidiser nozzles was 17.

In a conventional HF CCL, the oxidiser F_2 and primary fuel D_2 are supplied into the combustion chamber, the oxidiser is always being supplied in excess, so that the concentration ratio is $\alpha \equiv [F_2]/[D_2] > 1$. The value $\alpha = 1$ corresponds to the stoichiometric concentration ratio of the oxidiser and fuel. The excess fluorine almost completely dissociates at a high temperature achieved during the combustion of fluorine with deuterium. The temperature of combustion products depends on the content of the inert diluent He in the combustion chamber, which is determined (calculated with respect to free conditionally molecular fluorine remained after complete burning out of the primary fuel) by the parameter $\psi \equiv (\alpha - 1)^{-1}[He]/[D_2]$ (dilution degree). The high-temperature mixture is supplied from the combustion chamber to the laser zone through supersonic nozzles. Simultaneously, the secondary fuel H_2 is supplied through its channels to the nozzle unit. Its amount is characterised by the excess coefficient $R_L \equiv (\alpha - 1)^{-1}[H_2]/[D_2]$.

Below, we present the results of calculation for the fuel composition with parameters $\alpha = 1.4$, $\psi = 10$, $R_L = 35$, the oxidiser flow rate 0.36 g cm^{-2} s^{-1} per unit area of the nozzle array, and statistical pressure $p \sim 5$ Torr in the active medium near the nozzle unit exit plane.

To obtain simultaneous lasing in HF and HBr molecules, molecular bromine is injected into the secondary fuel flow, whose content in the mixture with H_2 is denoted by $\psi_{Br_2} \equiv [Br_2]/([H_2] + [Br_2])$. The addition of bromine leads to a strong increase in temperature due to the chain character of exothermal reactions proceeding in the mixture. The greatest additional heat release occurs in processes (5)–(8) with a high energy yield. As a result, temperature and pressure in the flow considerably increase, which causes its slowing down. This is illustrated in Fig. 2, where the level lines of the static pressure and temperature are shown in the

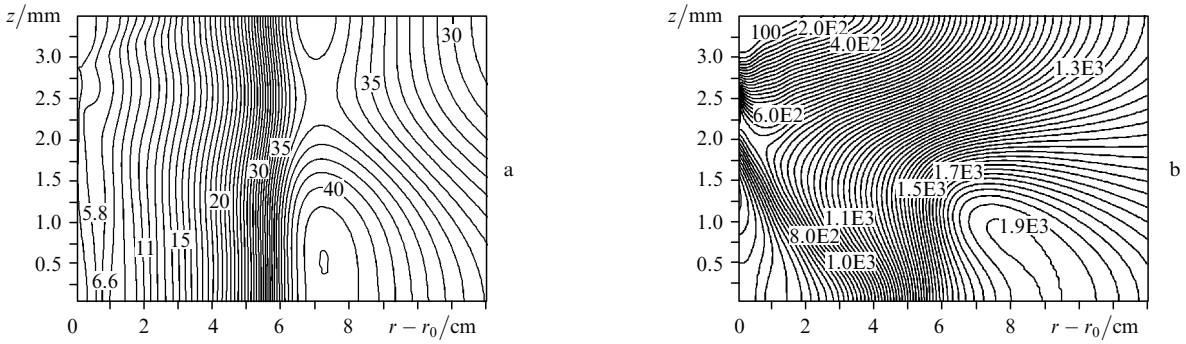

Figure 2. Level lines of static pressure (in torr) (a) and temperature (in kelvin) (b); $\psi_{Br_2} = 0.05$.

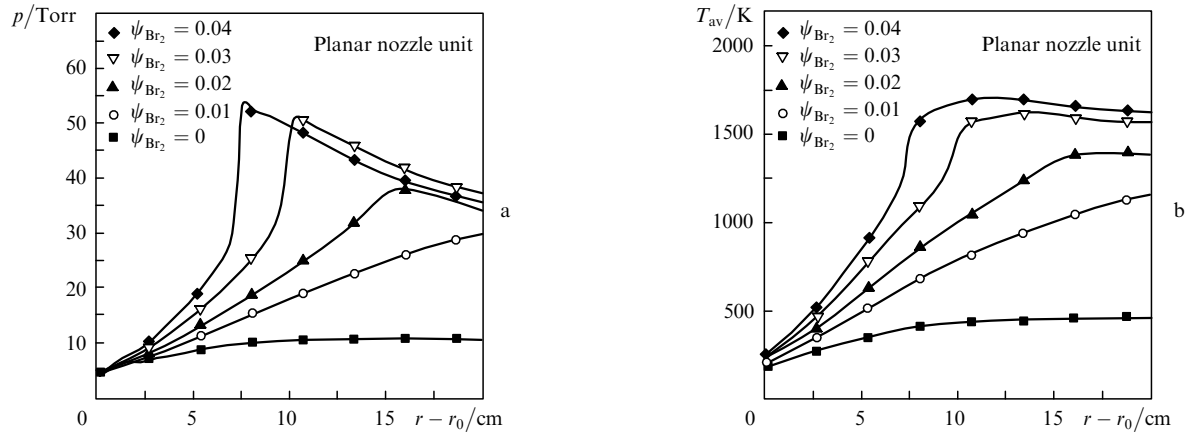

Figure 3. Distributions of static pressure p (a) and cross-section-averaged gas temperature T_{av} (b) for different degrees ψ_{Br_2} of dilution of the secondary fuel by bromine.

case of the 5 % dilution of the secondary fuel by bromine, i.e. for the molar ratio of fluorine and bromine equal to 1 : 1.75.

Figure 3 presents the distributions of the static pressure p and the cross-section-averaged gas temperature

$$T_{\mathrm{av}} = \int_0^{h^*} \rho V_r c_p T \mathrm{d}z \Big/ \int_0^{h^*} \rho V_r c_p \mathrm{d}$$

along the flow at the oxidiser nozzle axis for different degrees $\psi_{\mathrm{Br_2}}$ of dilution of the secondary fuel by bromine. The normal shock is distinctly observed for $\psi_{\mathrm{Br_2}} \geqslant 0.03$ at which the maximal local temperature $\sim$2050 K is achieved (the flow temperature without bromine does not exceed 900 K).

As the flow temperature increases, the amplification region becomes smaller and the small-signal gain (SSG) decreases. This is illustrated in Fig. 4 showing the distributions of SSGs (maximal over the rotational quantum number and averaged over the nozzle array period) at the vibrational frequencies of HF and HBr molecules for the undiluted secondary fuel (Fig. 4a) and for this fuel diluted by bromine by 4 % (Fig. 4b).

The amplification properties of the active medium at the vibrational frequencies of HBr molecules are optimal for $\psi_{\mathrm{Br_2}} \sim 0.02 - 0.04$, the maximum SSG being $\sim$0.015 cm^{-1} in the P_3 band. For $\psi_{\mathrm{Br_2}} > 0.04$, the amplification properties of the HBr laser are noticeably impaired due to a strong heat release and flow 'weighting'.

We studied also lasing for a planar nozzle unit with the active medium of length $L_{\mathrm{a}} = 50$ cm. The parameters of the Fabry–Perot resonator mirrors were assumed the same for all radiation frequencies and were chosen close to optimal parameters for the HBr laser: the reflectances of the mirrors were $r_1 = 0.99$, $r_2 = 0.925$, and the transmission coefficient of the output mirror was $t_2 = 0.07$ (the threshold gain was $g_{\mathrm{th}} = 9 \times 10^{-4}$ cm^{-1}).

Figure 5 shows the spectral intensity distributions in vibrational emission bands of HF and HBr molecules in the case of the 5 % dilution of the secondary fuel by bromine. One can see that the emission spectrum of HBr molecules contains more bands than that of HF molecules. Lasing was observed at the $P_1(7-12)$, $P_2(7-11)$, and $P_3(7-8)$ lines of HF molecules and at the $P_1(3-8)$, $P_2(4-11)$, $P_3(4-12)$, and $P_4(5-10)$ lines of HBr molecules.

Figure 6 presents the distributions of the intensities in different vibrational bands of HF and HBr molecules along the flow for $\psi_{\mathrm{Br_2}} = 0.04$. Figure 7 shows the dependences of the total output laser power P_{las} per unit nozzle array area and the lasing region length Δr_{las} at the vibrational frequencies of HF and HBr molecules on the degree of dilution of the secondary fuel by bromine. The emission power of

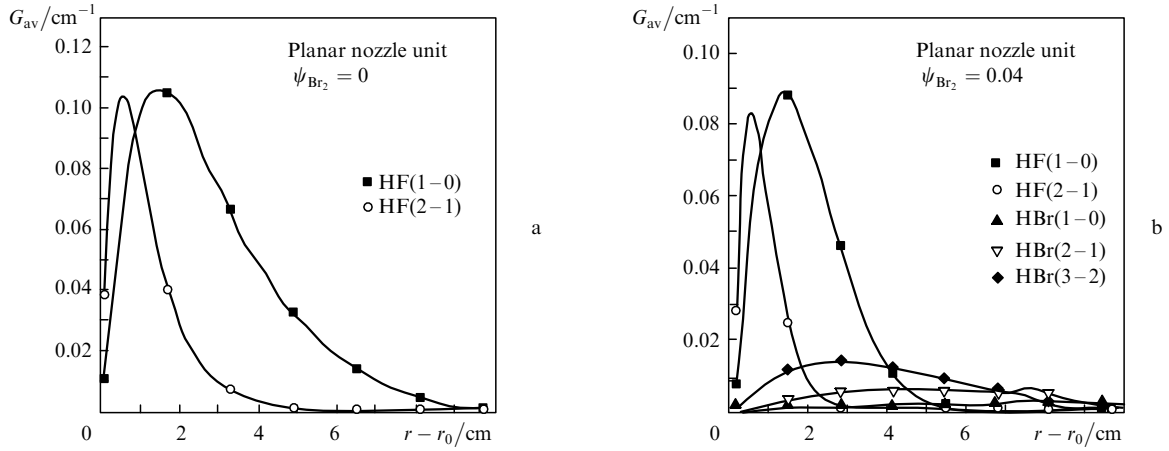

Figure 4. Distributions of SSGs G_{av} maximal over J and averaged over the nozzle array structure at vibrational frequencies of HF and HBr molecules for the undiluted secondary fuel (a) and the secondary fuel diluted by 4 % with bromine (b).

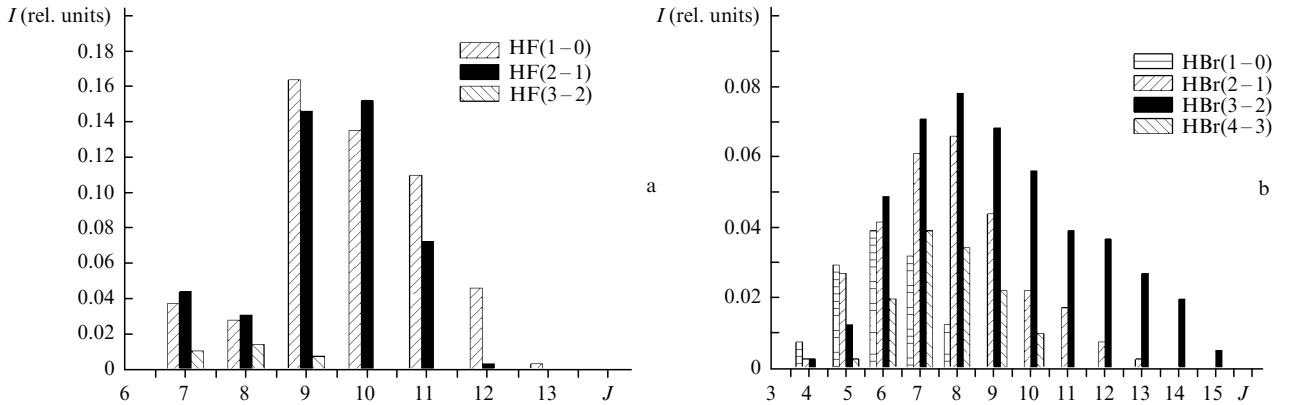

Figure 5. Spectral distributions of intensities in vibrational bands of HF (a) and HBr (b) molecules in the case of the secondary fuel diluted by 5 % with bromine.

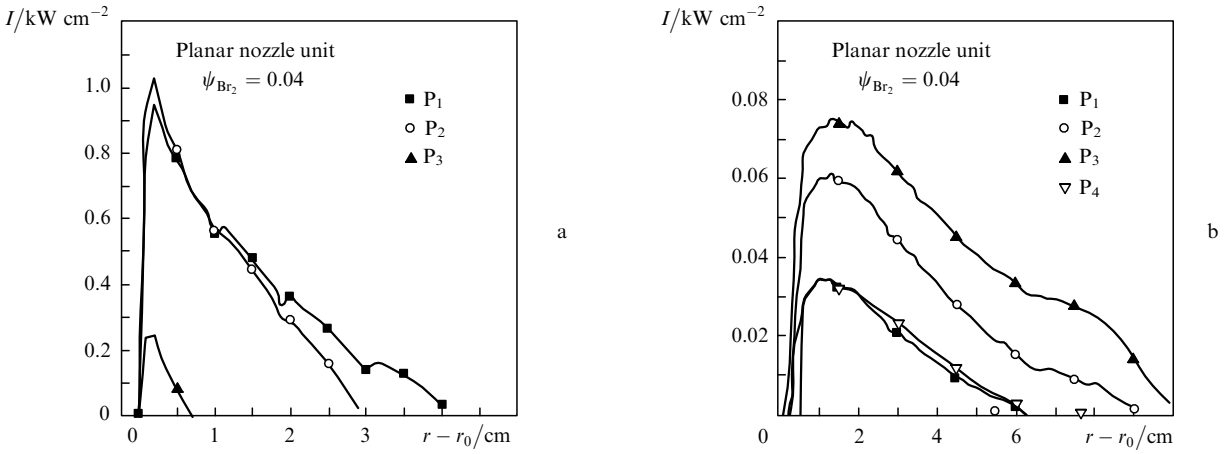

Figure 6. Distributions of the laser radiation intensity in different vibrational bands of Hf (a) and HBr (b) molecules.

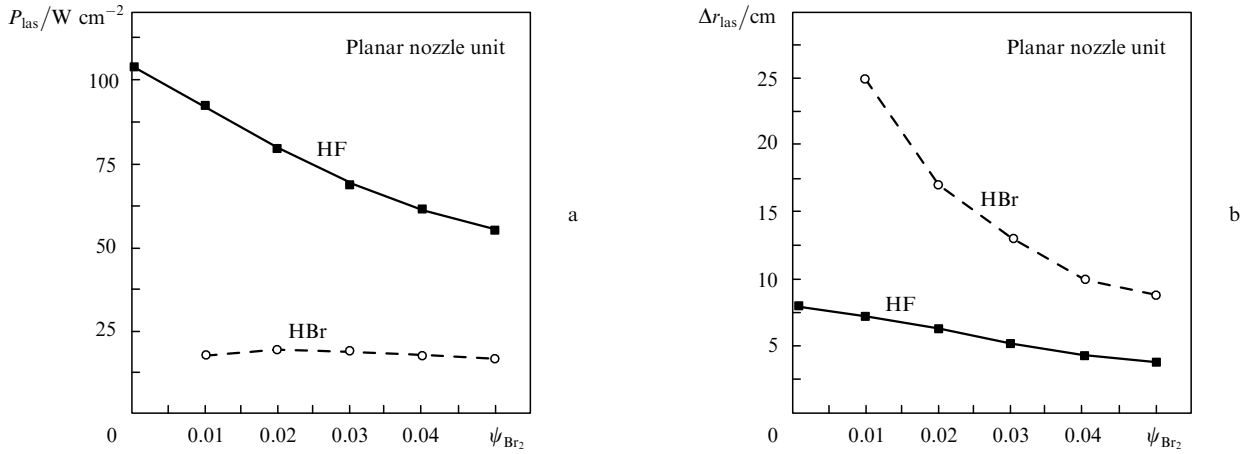

Figure 7. Dependences of the output power per unit nozzle array area P_{las} (a) and the laser region length Δr_{las} (b) for vibrational bands of HF and HBr molecules on the degree of dilution of the secondary fuel with bromine.

HBr molecules rather weakly depends on ψ_{Br_2} in the range from 0.01 to 0.04, and the maximum emission power density $\sim$20 W cm^{-2} is achieved for $\psi_{Br_2} \approx 0.02$.

The lasing region of the HBr laser is considerably longer than that of the HF laser due to a weaker relaxation of the vibrational states of HBr(v) molecules. For the optimal dilution degree $\psi_{Br_2} \approx 0.02$ providing the maximum output power, the length of the lasing region of the HBr laser is $\sim$15 cm. As ψ_{Br_2} is increased, the length of the lasing region for HF molecules decreases due to the increase in temperature and intensification of physicochemical processes in the active medium. In addition, the output power drastically

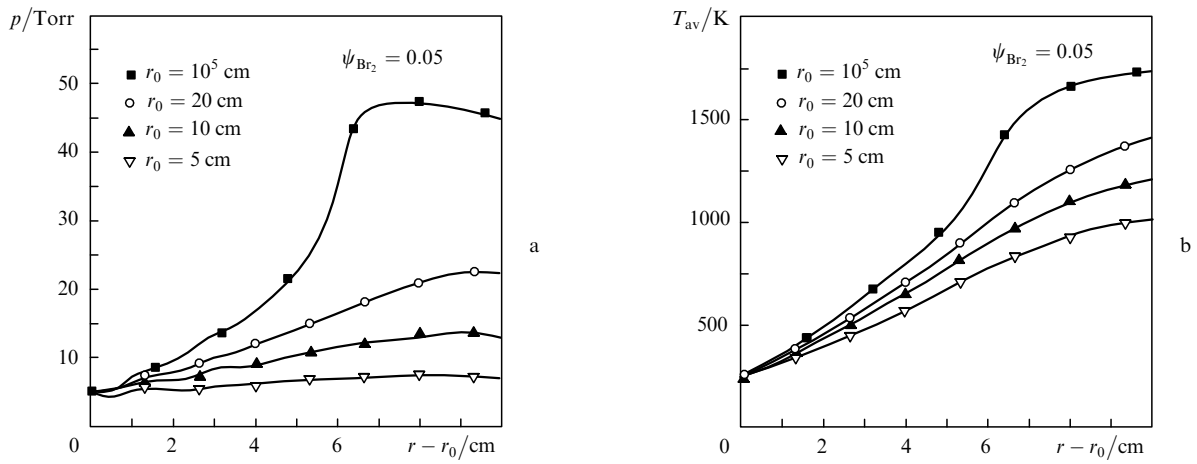

Figure 8. Distributions of static pressure p (a) and cross-section-averaged gas temperature T_{av} (b) for the 5% dilution of the secondary fuel with bromine at different cylinder radii r_0.

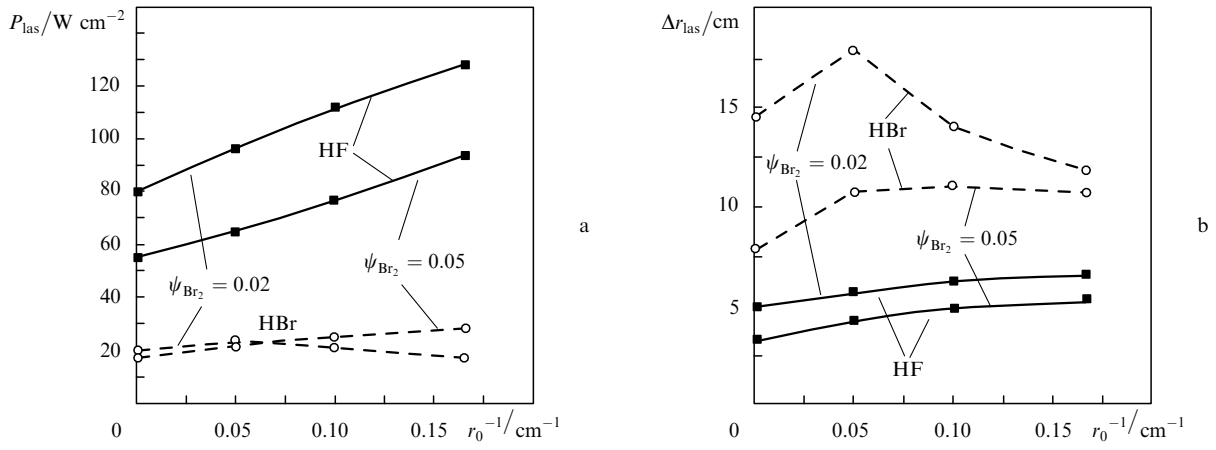

Figure 9. Dependences of the output power per unit nozzle array area P_{las} (a) and the laser region length Δr_{las} (b) on the nozzle unit curvature $1/r_0$ for different ψ_{Br_2}.

decreases. In particular, for $\psi_{Br_2} = 0.05$, the output power is half as much as that for $\psi_{Br_2} = 0$.

The pressure and temperature in the active medium can be decreased by transition from the planar nozzle unit construction to a cylindrical (or sector) design. Figure 8 shows the static pressure and averaged temperature distributions along the flow in the case of the 5 % dilution of the secondary fuel by bromine in the absence of radiation for several cylindrical generators with different radii r_0 on the nozzle unit. The replacement of the planar nozzle unit by the cylindrical design with $r_0 = 5$ cm reduces pressure in the lasing region by seven times and temperature by $\sim$1000 K. This improves the energy parameters of the laser.

Figure 9 presents the total output power per unit nozzle array area and the laser region length Δr_{las} for HF and HBr molecules as functions of the nozzle unit curvature $1/r_0$ for 2 % and 5 % dilutions for the resonator described above. On transition from the planar to cylindrical nozzle unit, the emission power of HF molecules increases independently of the dilution degree ψ_{Br_2}. The emission power of HBr molecules has a maximum at some curvature of the nozzle, which is displaced to lower values of r_0 with increasing ψ_{Br_2}.

4. Conclusions

(i) By solving complete Navier–Stokes equations describing the operation of a two-frequency HF–HBr CCL, we have obtained rather high reduced output powers at the vibrational frequencies of HBr molecules $P_{las} \sim 20$ W cm^{-2} for the laser region length $\sim$20 cm.

(ii) The ratio of radiation powers at $\lambda \sim 2.7$ μm (HF) and $\sim$4.2 μm (HBr) is controlled by the degree of dilution of the secondary fuel by bromine.

(iii) The replacement of the planar nozzle unit by the cylindrical (sector) unit considerably reduces pressure and temperature in the laser region. This noticeably improves the energy parameters of the laser.

(iv) A large difference between the lengths of lasing regions for HF and HBr molecules allows the use of two spatially separated resonators, which removes the problem of manufacturing broadband semitransparent resonator mirrors with the required parameters in two spectral ranges.

Acknowledgements. This work supported by the Russian Foundation for Basic Research (Grant No. 06-08-01335a).

References

1. Stepanov A.A., Shikanov V.A., Shcheglov B.A. *Kvantovaya Elektron.*, **8**, 765 (1981) [*Sov. J. Quantum Electron.*, **11**, 462 (1981)].
2. Martyshchenko V.V., Stepanov A.A., in *Trudy NPO 'Energomash'* (Proceeding of the Enegromash Research and Production Association) (Moscow: 2006) Vol. 24, pp 315–328.
3. Bashkin A.S., Gurov L.V., Katorgin B.I., et al., in *Trudy NPO 'Energomash'* (Proceeding of the Enegromash Research and Production Association) (Moscow: 2007) Vol. 25, pp 395–411.
4. Aleksandrov B.P., Beznozdrev V.N., Parfen'ev M.V., et al., in *Trudy NPO 'Energomash'* (Proceeding of the Enegromash Research and Production Association) (Moscow: 2007) Vol. 25, pp 423–434.
5. Aleksandrov B.P., Stepanov A.A., in *Trudy NPO 'Energomash'* (Proceeding of the Enegromash Research and Production Association) (Moscow: 2001) Vol. 19, pp 318–334.
6. Miller D.J., Shackleford W.L., Emanuel G. *Appl. Phys. Lett.*, **35**, 506 (1979).
7. Hirschfelder J.O., Curtiss C.F., Bird R.B. *Molecular Theory of Gases and Liquids* (New York: Wiley, 1954; Moscow: Inostrannaya Literatura, 1961).
8. Rotinian M.A., Strelets M.Kh., Shur M.L. *Proc. Int. Conf. on Laser Optics* (St. Petersburg, 1993).
9. Aleksandrov B.P., Stepanov A.A., in *Trudy NPO 'Energomash'* (Proceeding of the Enegromash Research and Production Association) (Moscow: 2007) Vol. 25, pp 435–448.
10. Aleksandrov B.P., Stepanov A.A. *Proc. SPIE Int. Soc. Opt. Eng.*, **6735**, 673509 (2007).
11. Aleksandrov B.P., Stepanov A.A., Shcheglov B.A. *Kvantovaya Elektron.*, **24**, 163 (1997) [*Quantum Electron.*, **27**, 158 (1997)].
12. Kovenya M.V., Yanenko N.N. *Metod rasshchepleniya v zadachakh gazovoi dinamiki* (Splitting Method in Gas-Dynamic Problems) (Novosibirsk; Nauka, 1981).
13. Cohen N.J., Bott J.F. *TR-0083(3603)-2* (El Segundo, Cal., The Aerospace Corp., 1982).